PHYSICAL REVIEW B, VOLUME 63, 081405(R)

n-alkyl thiol head-group interactions with the Au(111) surface

Y. Yourdshahyan, H. K. Zhang, and A. M. Rappe
Department of Chemistry and Laboratory for Research on the Structure of Matter, University of Pennsylvania, Philadelphia, Pennsylvania 19104-6323

(Received 18 August 2000; revised manuscript received 13 December 2000; published 6 February 2001)

State-of-the-art first-principles calculations based on density-functional theory were performed on $CH_3(CH_2)_{n-1}S$-Au(111) systems. We show that the adsorption site of methylthiolate at a range of coverages on the Au(111) surface is the fcc site, not the hcp site as has been recently reported. Further, we report that increasing alkane chain length enhances the fcc site preference. Study of the electronic structure of the system underscores the importance of sulfur 3*d* orbitals to thiol chemisorption.

DOI: 10.1103/PhysRevB.63.081405 PACS number(s): 68.43.−h, 71.15.Mb

The interaction between organic materials and solid surfaces has been extensively studied because of the broad range of industrial applications.[1–4] Self-assembled monolayers (SAM's) hold special interest, because the presence of the thiol group greatly strengthens the molecule-surface interactions, inducing order in the layer. SAM's have important potential applications in industry, such as sensors, transducers, detectors, packaging, and insulating layers for integrated circuits, functionalization of surfaces, thin coatings for electrodes, and corrosion inhibition.

The long-chain alkane thiols $[CH_3(CH_2)_{n-1}SH$, or $C_n]$ form SAM's on the Au(111) surface. Their simplicity, highly ordered structures, and chemical stability make these systems ideal for study with a variety of techniques including atomic-force microscopy,[5,6] infrared spectroscopy,[7,8] high-resolution electron-energy-loss spectroscopy,[9] grazing x-ray diffraction,[10] scanning tunneling microscopy,[11–16] scanning probe microscopy,[17] low-energy electron diffraction,[18–20] He atom diffraction,[21,22] and theory.[24–30] Despite extensive studies of this system, there are many controversies regarding its structure.

Two competing structural models, the ''standard model'' and the ''sulfur-pairing model,'' have considerable support. In the standard model, alkanethiol molecules exhibit a hexagonal $(\sqrt{3}\times\sqrt{3})R30°$ lattice. Alkanethiolates occupy threefold hollow sites of the Au (111) surface with S-S spacings of 4.99 Å, and the molecular axes are tilted by 30°–35° with respect to the surface normal.[13–16,18–22,29–34] The sulfur-pairing model involves a $c(4\times2)$ superlattice of the hexagonal lattice, where alkanethiolates form sulfur head group dimers with S-S spacings of 2.2 Å.[9–12,23–25] Furthermore, two theoretical studies have concluded that the adsorption site for a single thiol molecule on the gold (111) surface is the hcp hollow site.[29,30] However, despite the overall agreement of the results, there are discrepancies regarding the S-Au distance and the tilt of the molecule in these two independent studies.

Because the differences between these structures center around the thiol head-group locations, the investigation of the thiol-gold interaction is vital. Since interactions with the metal surface appear to dominate the molecular arrangement, many studies have focused on CH_3S on Au (111) as a prototype to study this entire class of SAM systems.

The main objective of our study is to identify the adsorption site for thiols on gold (111), and to explain the structural properties. We have performed first-principles calculations based on density-functional theory[35] (DFT) to study the adsorption of *n*-alkyl thiolates on the Au (111) surface. Our results show that thiol molecules adsorbed on the Au (111) surface with different coverages and chain lengths chemisorb on the fcc site. All of the first-principles calculations have been performed with the plane-wave pseudopotential code ''DACAPO.''[36]

In our DFT calculations, the wave functions are expanded in a plane-wave basis set, the electron-ion interactions are described by ultrasoft pseudopotentials (USPP),[37] and the generalized gradient approximation[38] for the exchange-correlation functional has been used. The Kohn-Sham equations are solved self-consistently, using a Pulay density-mixing scheme[39] to update the electronic density between iterations. The occupation numbers are updated using a recently developed technique based on minimization of the free-energy functional.[40] A finite electronic temperature is used, in order to reduce the number of *k* points needed, and all total energies are then extrapolated to zero electronic temperature.

When using the slab geometry in the plane-wave pseudopotential method, errors most often arise from the pseudopotential or from lack of convergence with respect to the number of *k* points, the cutoff energy, and the system size. When

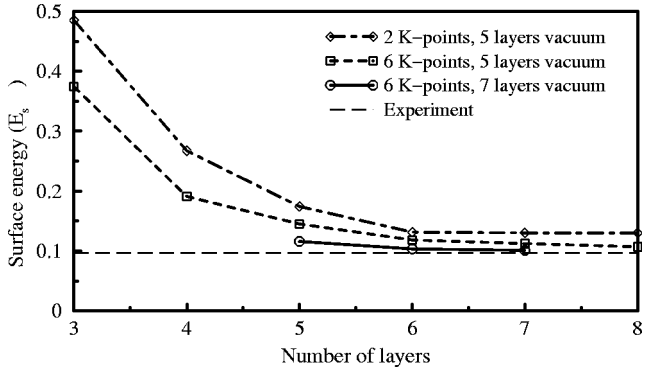

FIG. 1. The Au(111) surface energy in eV/Å^2 as a function of Au layers for different numbers of *k* points and vacuum thickness. All calculations are performed using a 30 Ry cutoff energy.

TABLE I. Structural and energetic results for the clean gold (111) surface (slab consists of 6 Au and 7 vacuum layers) and the CH_3S and CH_3SH molecules. Comparison of calculated results for the interlayer relaxations Δd_{12}, Δd_{23}, and Δd_{34} (1 = top layer) of the Au(111) surface. The presented distances are in Å and the surface energy (E_s) is given in eV/Å^2.

Clean Au (111) surface:				
	Δd_{12} (%)	Δd_{23} (%)	Δd_{34} (%)	E_s
This work	0.97	−0.48	0.07	0.101
Calc. (Ref. 45)	−0.24	0.05	0.04	0.084
Expt. (Ref. 46)	0.00			0.096
Optimized parameters for CH_3S:				
	r(CS)	$r(CH_a)$	$r(CH_b)$	$r(CH_c)$
This work	1.789	1.070	1.068	1.068
Calc. (Ref. 47)	1.799	1.095	1.091	1.091
	$\theta(SCH_a)$	$\theta(SCH_b)$	$\theta(SCH_c)$	$\phi(H_aSCH_b)$
This work	109.8°	110.7°	110.7°	116.3°
Calc. (Ref. 47)	107.0°	111.6°	111.6°	118.0°
Optimized parameters for CH_3SH:				
	r(CS)	r(CH)	$r(SH_d)$	$\theta(CSH_d)$
This work	1.827	1.08	1.36	97.2°
Expt. (Ref. 48)	1.819	1.09	1.34	96.5°

generating pseudopotentials it is important to preserve the eigenvalues for all relevant atomic configurations, not just in the reference configuration. However, in order to have correct lattice constants for metals it is also important to preserve the charge density in the tail region for all relevant atomic configurations.[43] We generated new USPP's for all elements involved, with maximum transferability errors less than 2 mRy.[44] All potentials are tested and compared to experiment and to all-electron calculations.

We find that although the $3d$ orbitals of S are nearly unpopulated in simple molecules, such as S_2, the d channel has great impact on the behavior of the pseudopotential. The $3d$ orbitals give S-enhanced polarizability and enable a great variety of bonding configurations through hybridization. A comparison between two USPP's for S with and without the d projector (transferability errors less than 2 mRy in both potentials) shows bond energies (E_b of S_2) of 2.51 and 3.08 eV/atom [all-electron and experimental values are 2.49 eV/atom (Ref. 41) and 2.37 eV/atom].[42]

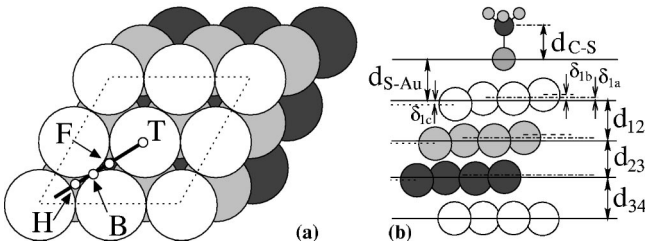

FIG. 2. Schematic presentation of the interaction of CH_3S with the Au(111) surface. T, H, B, and F denote top, hcp, bridge, and fcc sites, respectively. d_{xy} is the interlayer distance between layers x and y, where the top layer is denoted 1. δ_{xa} and δ_{xb} represent buckling for nearest and δ_{xc} for the next-nearest neighbors of the S atom.

In order to reduce calculation errors due to finite slab thickness, different slab geometries (3–8 layers thick) have been tested using different numbers of k points and vacuum layers (see Fig. 1). A slab consisting of $6+7$ Au+vacuum layers, a cutoff energy of 30 Ry, and a $4\times4\times1$ grid of special k points is found to give converged results (convergence within a few meV), which has been used for all calculations. Table I shows the equilibrium parameters for the clean Au (111) surface and the free CH_3S and CH_3SH molecules compared to experiment and other calculations.

The first step toward a detailed understanding of the SAM structure is to investigate the adsorption site of the simplest C_n (CH_3S) on the surface. Therefore, we calculated the total energy of a single CH_3S molecule in a (2×2) surface unit cell. As shown in Fig. 2(a), the thiolate was moved from top to fcc, then over the bridge to the hcp site using different molecular orientations. The three topmost Au layers and the

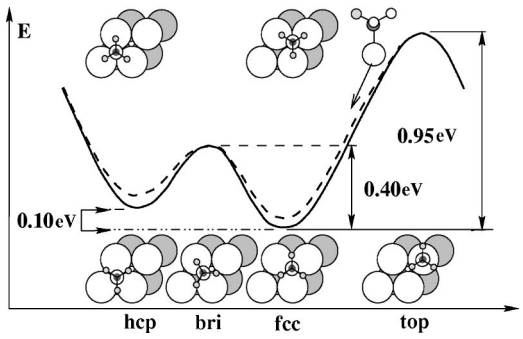

FIG. 3. The adsorption energy for a CH_3S molecule on the Au(111) surface along the diffusion path is shown. Small figures show top views for molecular orientation at each site. Solid and dashed lines represent energies for orientations shown below and above the curve, respectively.

TABLE II. Calculated parameters for CH_3S interaction with the Au (111) surface at 0.75 coverage. The parameters $d_{C\text{-}S}$, $d_{S\text{-}Au}$, and $d_{x,y}$ are the distances between the C and S atoms, between the S and the center-of-mass (CM) of the topmost Au layer, and the interlayer separation between the CM's of two adjacent layers. δ_{xa}, δ_{xb}, and δ_{xc} give the surface buckling.

	fcc	hcp	bri	top
ΔE_{chem} (eV)	0.00	0.10	0.40	0.95
$d_{S\text{-}Au}$ (Å)	1.788	1.831	1.990	2.493
d_{12} (Å)	2.399	2.398	2.430	2.410
d_{23} (Å)	2.386	2.382	2.398	2.379
d_{34} (Å)	2.393	2.389	2.401	2.398
δ_{1a} [δ_{2a}] (mÅ)	1[0]	5[0]	8[4]	15[10]
δ_{1b} [δ_{2b}] (mÅ)	4[2]	6[2]	7[5]	11[9]
δ_{1c} [δ_{2c}] (mÅ)	−3[−3]	−7[−3]	−8[−4]	−21[−13]
r(CS) (Å)	1.848	1.846	1.840	1.835
$r(CH_a)$ (Å)	1.105	1.105	1.106	1.106
$r(CH_{b,c})$ (Å)	1.104	1.104	1.105	1.106
$\theta(SCH_a)$ (deg)	108.6	108.7	108.9	109.1
$\theta(SCH_{b,c})$ (deg)	108.5	108.5	108.8	108.9

molecule were optimized using a damped molecular-dynamics method until the total force for the system was less than 0.01 eV/Å. Figure 3 shows calculated potential energy surfaces for two different molecular orientations along the diffusion path. The dashed curve is for the orientation used in Ref. 29 and the solid line is the minimum-energy path. Our results show that the staggered configuration is preferred over the configuration used in previous studies. The results of surface buckling and other optimization effects for the preferred orientation (solid line) are summarized in Table II and shown schematically in Fig. 2(b).

The calculated chemisorption energy difference between fcc and hcp, $\Delta E_{hcp\text{-}fcc}=0.10$ eV, shows that at low coverage CH_3S molecules adsorbed on the gold surface prefer the fcc site over hcp. This is in contrast with results of Refs. 29 and 30, which are based on cluster calculations and classical MD. In the cluster calculations, only two gold layers were used. As a result, the surface energy is far from converged, and the effect of gold atoms in the third layer is not included. As can be seen from Fig. 1, the gold (111) surface energy is converged only when six or more gold layers are used. Furthermore, the energy difference between having the molecule at the fcc or hcp sites, ($\Delta E_{hcp\text{-}fcc}$) increases from 0.04 to 0.10 eV as the slab thickness is increased from four to six gold layers. This indicates the importance of slab size and suggests that the use of a two-layer gold slab is insufficient for accurate results.

Our investigations of chain length and coverage show that the fcc site preference is robust. Moving from CH_3S to two-, three- and seven-carbon thiols increases the energy difference, $\Delta E_{hcp\text{-}fcc}$, to 0.150, 0.180, and 0.185 eV. These results indicate that the preference for fcc becomes stronger with increasing number of carbons in the chain. Our investigation also indicates that the fcc site is the preferred position for a range of coverages. The energy differences, $\Delta E_{hcp\text{-}fcc}$, of 0.099, 0.100, 0.102 eV for coverages 0.25, 0.75, and 1 (per $\sqrt{3}\times\sqrt{3}R30°$ unit cell) clearly show that coverage does not affect site preference.

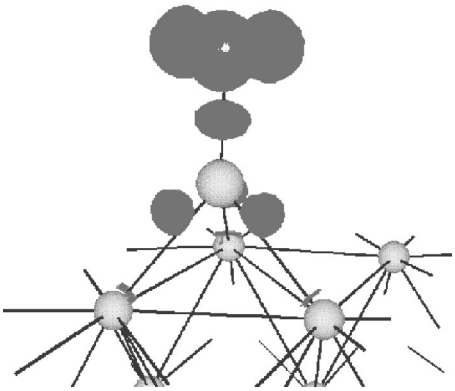

FIG. 4. Showing a 3D isosurface of calculated induced charge density (with a value of 0.1 e/Å^3) when the methylthiolate is adsorbed on the fcc site.

The induced charge-density isosurface plot (Fig. 4) illustrates the bonding between the thiolate and the gold (111) surface. The induced charge density (the charge density of the chemisorbed system minus that of the slab and molecule) shows a build-up of charge between the sulfur atom and each of the three nearest gold atoms, representing chemisorption bonds. It is important to note that the C-S-Au bond angles are all between 132° and 138°, significantly larger than the tetrahedral angle of 109 degrees. This effect can be attributed to Pauli repulsion between the sulfur atom and the delocalized metallic electrons in the gold. Further evidence of this effect is found in the induced charge density itself. The maxima of induced charge do not lie on the S-Au internuclear axis; they are shifted away from the surface. The polarizability of the sulfur atom and the accessibility of delocalized states in the metal make possible this unconventional arrangement of bonding electrons.

In summary, we have presented state of the art DFT calculations of thiol molecules adsorbed on the Au (111) surface at different coverage. This study demonstrates that the fcc site is the preferred location for a single thiol, and the electronic changes which accompany chemisorption are elucidated. The effect of hydrocarbon chain length and coverage were also investigated, showing the same preferred headgroup adsorption site (fcc) in all cases. Furthermore, the importance of having a minimum of six gold layers in the model, and of including *d* orbitals in the sulfur pseudopotential were highlighted.

The authors wish to acknowledge G. Scoles for his insightful comments concerning this subject. This work was supported by NSF grant DMR 97-02514 and the Air Force Office of Scientific Research, Air Force Materiel Command, USAF, under Grant No. F49620-00-1-0170. AMR would like to thank the Camille and Henry Dreyfus Foundation for support. Computational support was provided by the National Center for Supercomputing Applications and the San Diego Supercomputer Center.

[1] A. Ulman, *An Introduction to Ultrathin Organic Films* (Academic, Boston, 1991).
[2] R. Maboudian, Surf. Sci. Rep. **30**, 207 (1998).
[3] P.A. DiMilla *et al.*, J. Am. Chem. Soc. **116**, 2225 (1994).
[4] O. Chailapakul, L. Sun, C. Xu, and M.R. Crooks, J. Am. Chem. Soc. **115**, 12 459 (1993).
[5] K. Tamada, M. Hara, H. Sasabe, and W. Knoll, Langmuir **13**, 1558 (1997).
[6] S. Xu *et al.*, J. Chem. Phys. **108**, 5002 (1998).
[7] C.D. Bain and G.M. Whitesides, J. Am. Chem. Soc. **111**, 7164 (1989).
[8] R.G. Nuzzo, E.M. Korenic, and L.H. Dubois, J. Chem. Phys. **93**, 767 (1990).
[9] G.J. Kluth, C. Carraro, and R. Maboudian, Phys. Rev. B **59**, R10 449 (1999).
[10] P. Fenter, A. Eberhardt, and P. Eisenberger, Science **266**, 1216 (1994); P. Fenter, A. Eberhardt, K.S. Liang, and P. Eisenberger, J. Chem. Phys. **106**, 1600 (1997).
[11] G.E. Poirier and M.J. Tarlov, J. Phys. Chem. **99**, 10 966 (1995).
[12] N. Camillone *et al.*, J. Chem. Phys. **99**, 744 (1993).
[13] F.T. Arce, M.E. Vela, R.C. Salvarezza, and A.J. Arvia, Langmuir **14**, 7203 (1998).
[14] R. Yamada, H. Wano, and K. Uosaki, Langmuir **16**, 5523 (2000).
[15] H. Kondoh and H. Nozoye, J. Phys. Chem. B **103**, 2585 (1999).
[16] M.D. Porter, T.B. Bright, D.L. Allara, and C.E.D. Chidsey, J. Am. Chem. Soc. **109**, 3559 (1987).
[17] C.A. Alves, E.L. Smith, and M.D. Porter, J. Am. Chem. Soc. **114**, 1222 (1992).
[18] N. Camillone *et al.*, J. Chem. Phys. **101**, 11 031 (1994).
[19] L.H. Dubois, B.R. Zegarski, and R.G. Nuzzo, J. Chem. Phys. **98**, 678 (1993).
[20] C.E.D. Chidsey and D.N. Loiacono, Langmuir **6**, 709 (1990).
[21] N. Camillone, C.E.D. Chidsey, G. Liu, and G. Scoles, J. Chem. Phys. **98**, 3503 (1993).
[22] C.E.D. Chidsey, G. Liu, P. Rowntree, and G. Scoles, J. Chem. Phys. **91**, 4421 (1998).
[23] N. Nishida, Y. Hara, H. Sasabe, and W. Knoll, Jpn. J. Appl. Phys., Part 2 **35**, L799 (1996); **35**, 5866 (1996).
[24] R. Bahatia and B.J. Garrison, Langmuir **13**, 4038 (1997).
[25] J.J. Gerdy and W.A. Goodard, J. Am. Chem. Soc. **118**, 3233 (1996).
[26] W. Mar and M.L. Klein, Langmuir **10**, 88 (1994).
[27] A.J. Pertsin and M. Grunze, Langmuir **10**, 3668 (1994).
[28] M.C. Vargas, P. Giannozzi, A. Selloni, and G. Scoles (unpublished).
[29] H. Sellers, A. Ulman, Y. Shnidman, and J.E. Eilers, J. Am. Chem. Soc. **115**, 9389 (1993).
[30] K.M. Beardmore, J.D. Kress, N. Gronbech-Jensen, and A.R. Bishop, Chem. Phys. Lett. **286**, 40 (1998); Synth. Met. **84**, 317 (1997).
[31] H.A. Biebuyck, C.D. Bain, and G.M. Whitesides, Langmuir **10**, 1825 (1994); C.D. Bain, H.A. Biebuyck, and G.M. Whitesides, *ibid.* **5**, 723 (1989).
[32] K.T. Zhong, R.C. Brush, Anderegg, and M.D. Porter, Langmuir **15**, 518 (1999).
[33] R.G. Nuzzo, B.R. Zegarski, and L.H. Dubois, J. Am. Chem. Soc. **109**, 733 (1987).
[34] K.T. Carron and G.J. Hurley, J. Phys. Chem. **95**, 9979 (1991).
[35] W. Kohn and L.J. Sham, Phys. Rev. **140**, A1133 (1965); **145**, A561 (1966).
[36] L. Hansen *et al.*, computer code DACAPO-1.30, CAMP, DTU, Denmark.
[37] D. Vanderbilt, Phys. Rev. B **41**, 7892 (1990).
[38] J.P. Perdew, K. Burke, and M. Ernzerhof, Phys. Rev. Lett. **77**, 3865 (1996).
[39] G. Kresse and J. Furthmüller, Comput. Mater. Sci. **6**, 15 (1996).
[40] L. Bengtsson, Ph.D. thesis, Chalmers University of Technology, Göteborg, Sweden, 1999.
[41] Xi Lin (private communication).
[42] K.P. Huber and G. Herzberg, *Molecular Spectra and Molecular Structure* (Van Nostrand Reinhold, New York, 1979), Vol. 4.
[43] I. Grinberg, N.J. Ramer, and A.M. Rappe (unpublished).
[44] For H ($1s^1$), C ($2s^2 2p^2$), S ($3s^2 3p^{3.5} 3d^{0.5}$), and Au ($5d^{9.5} 6s^1 6p^{0.5}$) the USPP's were generated using cutoff radii (r_c) of 0.60, 1.24, 1.45, and 2.00 bohr, respectively.
[45] H. Cox, X. Liu, and J.N. Murrell, Mol. Phys. **93**, 921 (1998).
[46] M.A. Van Hove, and S.Y. Tong, *Crystallography by LEED* (Springer, Berlin, 1976).
[47] S.W. Chiu, W.K. Li, W.B. Tzeng, and C.Y. Ng, J. Chem. Phys. **97**, 6557 (1992).
[48] Data taken from CRC handbook.